PROCEEDINGS, 50th Workshop on Geothermal Reservoir Engineering
Stanford University, Stanford, California, February 10-12, 2025
SGP-TR-229

Exploring Low-Temperature Geothermal Systems in Hydrocarbon-Bearing Sedimentary Basins: A Case Study from the Czech Vienna Basin

Rybár, S.[1,2] Nemčok, M.[1,3] Kyselák, P.[4] Ledvényiová, L.[1] and Sliva, Ľ.[5]

1 Faculty of Mining and Geology, VŠB-Technical University of Ostrava, 17. listopadu 15, 708 00 Ostrava, Czech Republic

2 Department of Geology and Paleontology, Comenius University, Ilkovičova 6, Bratislava 842 15, Slovakia

samuelrybar3@gmail.com

3 RM Geology, Donská 38, 841 06 Bratislava, Slovakia

4 MND, a.s., Úprkova 6, 695 01 Hodonín, Czech Republic

5 NAFTA a.s., Plavecký Štvrtok 900, 900 68 Plavecký Štvrtok, Slovakia

Keywords: Low-Temperature Geothermal Systems, Vienna Basin, Hydrocarbon-Bearing Sedimentary Basins, Fault-Controlled Fluid Flow

ABSTRACT

The future of geothermal energy development increasingly focuses on low-temperature geothermal systems within hydrocarbon-bearing sedimentary basins. This study investigates the geothermal potential of the Czech sector of the Vienna Basin, a pull-apart basin that continued evolving under back-arc extension. The Czech portion occupies the northeastern acute corner of the basin, separated from the Slovak sector by the Hodonín-Gbely Horst. The study identifies four groups of horizons belonging to four stratigraphies as potential geothermal aquifers: the lower Badenian (lower Langhian), middle Badenian (upper Langhian), upper Badenian (lower Serravallian), and Sarmatian (upper Serravallian). The lower Badenian strata appear to be the least significant in terms of geothermal potential. The aforementioned stratigraphies correspond to different evolutionary stages of the basin, with the lower Badenian possibly deposited during the initial phase of pull-apart formation, while the middle Badenian marks the mature stage with the development of a regional depocenter. The upper Badenian and Sarmatian intervals were deposited during the subsequent phase of back-arc extension (wide-rift setting), characterized by the reactivation of boundary sinistral strike-slip fault zones as normal faults. Preliminary results indicate a topography-driven fluid flow system with recharge area occurring along the northwestern margin, along the basin-bounding Steinberg Fault Zone and discharge area along the hanging wall of the Lužice-Lanžhot Fault Zone which separates the Central Moravian Sub-basin from the Hodonín-Gbely Horst. The temperature difference between recharge and discharge areas is 18 °C at the depth of 1 km. The assessment of total dissolved solids suggests a heterogeneous hydrogeological system, with multiple interconnected aquifers exhibiting varying degrees of fluid mineralization. Given the relatively low geothermal gradient, utilization of geothermal fluids for electricity generation is unlikely. However, the identified geothermal reservoirs hold significant potential for direct applications, including district heating, greenhouse agriculture, aquaculture, and spa-related tourism. Future research will focus on refining reservoir characterization through seismic data analysis supported by modeling, to optimize geothermal utilization strategies in the region.

1. INTRODUCTION

Geothermal energy is gaining recognition as a key renewable and sustainable energy resource with the potential to significantly contribute to the global energy transition (Jamil et al., 2023). Geothermal energy consumption and technological innovations are proven to contribute to a reduction in CO_2 emissions, in contrast to nonrenewable energy consumption, which exacerbates these emissions (Idroes et al., 2024). Beyond its environmental benefits, geothermal energy serves as a bridge in the transition from fossil fuels, supporting local energy production and promoting social development (Bjornsson et al., 2024). Recently, low-temperature geothermal systems have attracted increasing attention (e.g. Brown and Falcone 2024), particularly in hydrocarbon-bearing sedimentary basins (e.g. Majorowicz and Grasby 2019). Low-temperature geothermal systems utilize geothermal reservoirs with temperatures below 150 °C (Sanyal, 2005). Low-temperature geothermal resources hold immense potential for direct applications in residential, commercial, industrial, and agricultural sectors, including space and water heating, greenhouse warming, aquaculture, and low-temperature manufacturing processes (e.g. Mullane et al., 2016; Skrzypczak et al., 2021; Knezevic et al., 2023; Sachsenhofer et al., 2023). Moreover, innovative hybrid systems integrating geothermal energy with other energy sources are being explored to enhance electricity production in low-temperature geothermal areas (e.g. Kohla and Speck, 2004).

The energy transition has also driven interest in repurposing abandoned oil wells for geothermal energy exploration. The Hammam Faraun geothermal site in Egypt exemplifies how abandoned oil well logs, seismic data, and surface geology can be utilized to evaluate geothermal resources. At this site, seismic interpretation identified significant fault systems that enable a renewable geothermal cycle through the circulation of mixed formation and sea waters (Shawky et al., 2024). Vienna Basin (Figure 1) represents a promising, yet underexplored, region for low-temperature geothermal systems, particularly in the Czech and Slovak parts. Historically, geothermal waters have been identified in coarse clastic reservoirs of Badenian and Sarmatian (Langhian/Serravalian) age. Despite these findings, detailed studies of low-temperature geothermal systems in the Czech and Slovak parts are scarce, with the majority of available research focusing on the Austrian part. For instance, recent studies in the Schwechat sub-basin identified low-velocity anomalies beneath Vienna, suggesting the presence of water-saturated open cracks that may offer geothermal exploration opportunities (Esteve et al., 2025).

Despite the relatively low-thermal characteristics of the Vienna Basin (Boldizsár, 1968; Franko et al., 1995), the geological, seismic, and well data gathered during previous hydrocarbon extraction activities serve as critical resources for assessing its geothermal potential. Notably, the Czech portion of the basin exhibits promising conditions for geothermal development, creating opportunities for comprehensive geological, hydrological, and thermal evaluations.

Consequently, based on previously unpublished geo-seismic lines, this study aims to address these critical knowledge gaps by focusing on the geothermal potential of the Czech Vienna Basin. The main objectives are as follows: To analyze the geothermal potential of stratigraphic intervals in the Czech Vienna Basin. To evaluate the role of fault systems and structural highs in controlling fluid flow. To assess recharge and discharge areas as indicators of geothermal activity.

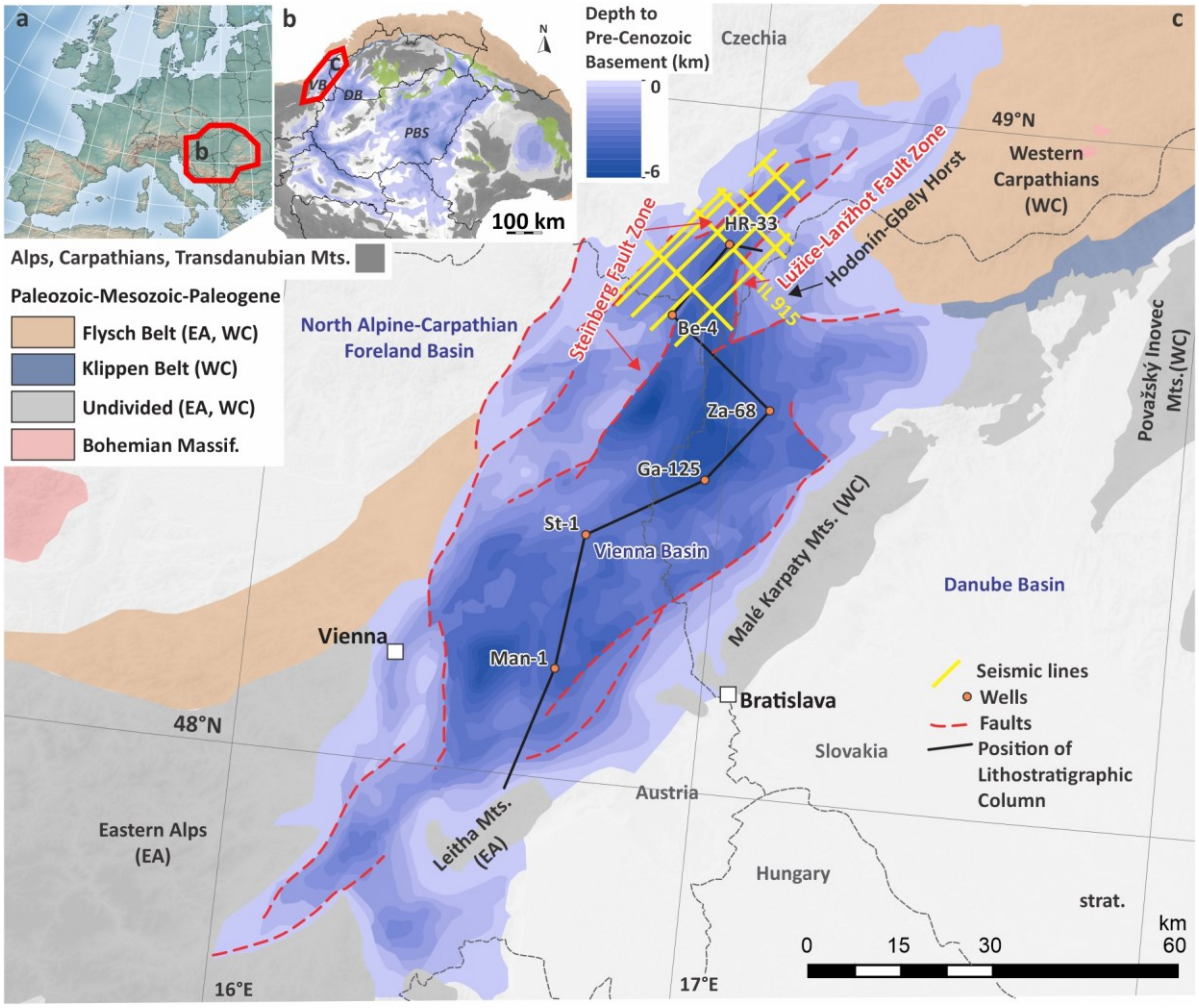

Figure 1: Position of the Vienna Basin within a) in Europe and b) within the Alpine–Carpathian–Pannonian region.

2. GEOLOGICAL SETTING OF VIENNA BASIN (VB)

2.1 Structure

The Early Miocene development of the area proceeds in and piggy-back (Lee and Wagreich, 2017) basin stage, possibly as part of the closing Alpine-Western Carpathian foreland. During the early Badenian (early Langhian)(Figure 2), the immature stage of the pull-apart basin takes place, which is detached at brittle deformational level, and the topography of which starts to overprint the pre-existing Alpine-Carpathian orogen and its foreland. This is most likely the time when local depocenters are divided by a number of structural highs including the Hodonín-Gbely Horst, which separates the Czech and Slovak sectors of the basin, is fully differentiated During the middle Badenian (late Langhian) the mature stage of the pull-apart basin develops (Jelínek et al., 2009; Nemčok et al., 2024), characterized by the occurrence of a regional depocenter superposed on a system of former depocenters, The upper Badenian and Sarmatian (Serravallian) strata are deposited during the evolution of the basin under the regional back-arc extension, reactivating former boundary strike-slip fault zones or even older basement related thrust faults and reforming them to low angle normal fault zones typical for the Wide-rift setting (Matenco and Radivojević, 2012) or equivalently Basin and Range setting (Osborn, 2024). The wide-rifting possibly continues into the early Pannonian (Tortonian) (Harzhauser et al., 2024). The late Pannonian is characterized by post-rift thermal subsidence and basin inversion (Lee and Wagreich, 2017).

2.2 Stratigraphy

In the southern and central parts, the pre-Neogene basement of the VB includes granitoide crystalline units overlain by Alpine-Carpathian Paleozoic to Mesozoic cover and nappe units, composed mainly of Mesozoic carbonates. In the North and Northwest, including the entire Czech segment the basin, the basement is represented by upper Cretaceous to Miocene rocks belonging to the Western Carpathian Flysch belt accretionary prism (Fusán et al., 1987; Hók et al., 2014, 2022). The older basin fill starts with Lower Miocene shelf-deposited mudstone and sandstone to conglomerate (in the south passing into brackish lake condition at the end of the Burdigalian) intercalations deposited in the epicontinental Paratethys Sea (Vass, 2002; Harzhauser et al., 2020, 2024), transitioning into the younger Middle/Late Miocene basin fill occupied mostly by calcareous mudstones, limestones and coarse clastics accumulated predominantly during the Badenian transgression (Vass, 2002; Fordinál et al., 2013; Harzhauser et al., 2019). The Sarmatian is characterized by calcareous mudstone with sand layers, indicating marine to deltaic and continental environments. Subsequent sedimentation reflects the transition to the brackish/freshwater Lake Pannon, with the deposition of sands, mudstones, and lignite layers (Vass 2002) (Figure 2).

2.3 Hydrogeology

In the Vienna Basin, the chemical composition of groundwater primarily reflects its original sedimentary environment, though it has been partially modified by interactions with fossil waters, rock formations, organic matter, and dissolved gases (Janák 1955). The Paleozoic, Mesozoic, and Paleogene pre-basin strata, along with the Lower Miocene basin fill, contain brackish to saline waters with total dissolved solids (TDS) ranging from approximately 3,000 to 30,000 ppm, indicative of generally open structures (Janák 1955; Michalíček 1971; Němec & Kocák 1976). Notable exceptions occur in the Triassic deposits, where high-salinity brines influenced by sabkha evaporite layers can reach mineralization levels between 90,000 and 130,000 ppm TDS (Dlabač et al. 1968). However, these deposits are absent in the Czech portion of the basin. The Karpatian (upper Burdigalian) aquifers exhibit low mineralization, reflecting a transition from a brackish lake to a fluvial depositional setting. Despite this reduced salinity, these structures are likely to be closed to significant extent (Michalíček 1971). Badenian aquifers typically contain saline marine waters with TDS concentrations between 12,000 and 30,000 ppm, suggesting mostly closed hydrogeological structures. In contrast, Sarmatian sediments show a decline in mineralization to brackish or near-normal salinity, with a maximum of 20,000 ppm TDS, reflecting shifts in paleoenvironmental conditions and predominantly closed structures. Pannonian waters are generally brackish, with TDS levels reaching up to 13,000 ppm, gradually transitioning to fresher waters at shallower depths, indicative of more open structures (Janák 1955; Dlabač et al. 1968; Michalíček 1971; Němec & Kocák 1976). The Vienna Basin exhibits a relatively low geothermal gradient compared to neighboring basins. At depths of approximately 1,000 meters, temperatures typically range between 50 °C and 60 °C, while at intermediate depths around 3,000 meters, they generally range from 100 °C to 120 °C. The average regional heat flow is moderate, reaching about 55 mW/m² (Franko et al. 1995).

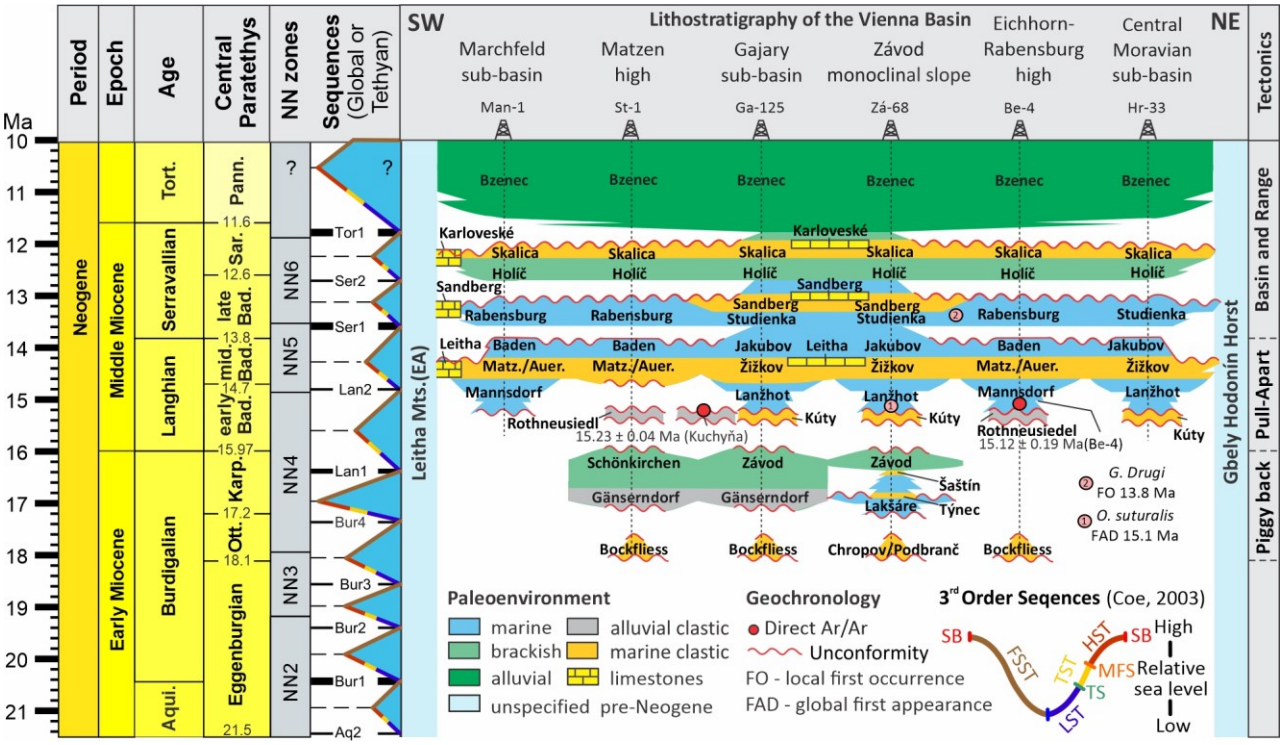

Figure 2: Miocene Chrono/lithostratigraphic framework of the Vienna Basin and the location map of studied sections. Timescale is adapted from Krijgsman and Piller (2012); the lithostratigraphic details follow Špička (1966), Vass (2002), Kováč et al. (2008), Fordinál et al. (2013), Harzhauser et al. (2019, 2020,2024), global sequences are after Haq et al. (1988) and Hardenbol et al. (1998), Coe (2003); FAD - *O. suturalis* from Wade et al. (2011), FO *G. druryi* after Hudáčková et al. (2013), Šarinová et al. (2021); Ar/Ar dating after Rybár et al. (2019) and Sant et al. (2020).

3. MATERIALS AND METHODS

Besides the review of published scientific papers, monographs and reports, previously unpublished reflection seismic line interpretations were used in this study In particular, we analyzed 10 arbitrary line extractions from modern high-quality 3D volumes. One of them is presented in this study. Velocity measurements for this study were available in the form of 16 key well check shots, which were loaded into the Petrel software. With respect to the well data, multiple wells were projected onto the presented geo-seismic profile (IL 915) and used for seismic horizon interpretation.

Paleoenvironemental nomenclature followed the framework established by Pellegrini et al. (2020). The structural architecture of the basin was assessed based on the studies of Matenco and Radivojević, (2012) and Osborn (2024). Seismic and sequence stratigraphic interpretations of reflection seismic profiles were done using the methodology described by Brown and Fisher (1980), Coe (2003) and Fischer and Veeken (2015). The presented geo-seismic profile IL915 is located in the central part of the Czech sector of Vienna Basin. It represents on NW – SE cross-section cutting through the entire Central Moravian sub-basin. Based on the provided seismic header file, the analyzed Profile IL915 represents a 2D profile extracted from a larger 3D volume. It was acquired with a sample interval of 2 ms and a recording length of 4 seconds (2000 samples per trace). The data were recorded in IBM floating-point format, with each trace header containing shotpoint (byte position 17), CDP (byte position 21), and source-receiver coordinates (byte positions 73–80 for X and Y). A coordinate scale factor of 1 was applied. The fold of coverage is 1, indicating single-fold seismic data. Source and receiver locations were automatically detected, and the survey geometry adheres to acquisition practices. These parameters ensure adequate resolution and spatial coverage for evaluating the structural and stratigraphic features in the study area.

The targeted stratigraphic intervals for geothermal analysis in the case of this presented profile are 1) middle Badenian (upper Langhian), upper Badenian and Sarmatian (Serravallian) aquifers – as they include the largest volume of well data including perforations with fluid geochemistry analyzes see Ledvényiová et al., (2025)

in this wolume for more info on fluids. The findings of this study should be understood in light of several data limitations. Although the Central Moravian Sub-basin is almost entirely covered by 3D reflection seismic data, the dataset available for this study was restricted to the mentioned 10 arbitrary seismic profiles, supplemented by limited well data. Moreover, petrophysical data were not available for this analysis.

4. RESULTS

4.1 Fault Systems and Structural Highs

The most prominent structural feature in the northwestern part of the presented seismic profile is a low-angle normal fault with a SW-NE strike and SE dip, forming the basin margin. Multiple smaller faults with similar strike and dip occur along this structure, forming tilted fault blocks that detach and slip basin-ward. Together, these faults create a fault zone referred to as the Steinberg Fault Zone, which is observed to extend upwards at least to the Pannonian (Tortonian) strata, and possibly higher (Figure 3).

In the southeastern section of the profile, a significant offset along the low-angle normal fault has resulted in the development of a major detachment surface, which separates a tilted fault block known as the "Gbely-Hodonín Horst" from the basin fill. This structure forms a prominent basement high, being over 10 km wide. The horst is bounded by an antithetic normal fault with a SW-NE strike and a NW dip, opposing the low-angle normal fault. The antithetic fault zone comprises multiple branching faults, which create additional tilted fault blocks, collectively referred to as the Lužice-Lanžhot Fault Zone (Figure 3).

The internal structure of the basement high can also be partially described. It appears to include two detachment horizons: one located between the Paleogene basement and Lower Miocene intervals, and a second between the Lower and Middle Miocene intervals. The latter detachment seemingly continues into the antithetic fault zone. The Lower Miocene intervals are deformed by a set of normal faults rooted in the detachment, which do not extend above the base of the Middle Miocene strata (Figure 3).

Faults within the antithetic normal fault zone extend upwards, reaching as high as the Pannonian strata and, occasionally, even to the surface. The lower and middle Badenian intervals exhibit characteristics of sag-fill deposits, while the Sarmatian and Pannonian intervals display clear thickening towards the low-angle normal fault. Notably, the Sarmatian marks the time when the basement high, the Gbely-Hodonín Horst, was completely buried (Figure 3).

4.2 Stratigraphic and Reservoir Characteristics:

Through the analysis of three seismic sequences, comprising a total of nine seismic facies, six key intervals with potential for geothermal activity have been identified.

The middle Badenian Seismic (upper Langhian) sequence (MBS), the oldest sequence analyzed, begins above an erosional surface observable along the northwestern margin of the basin (Figure 3). This sequence is characterized by downlap terminations at its base and concordances at its top. It can be further subdivided into at least four distinct seismic facies:

Seismic Facies 1 (Sf1) corresponds directly to **Interval of Interest 1 (Ii1).** It is characterized by predominantly parallel to occasionally subparallel continuous reflections, which are frequently interrupted by normal faults. The reflections exhibit generally high amplitudes, and the frequency is predominantly broad.

Seismic Facies 2 (Sf2) is represented by an interval characterized by indistinct prograding clinoforms, transitioning into subparallel, discontinuous reflections. These reflections are predominantly of low amplitude and exhibit variable frequency. The facies is extensively disrupted by numerous normal faults.

Seismic Facies (Sf3) represents the second **Interval of Interest 2 (Ii2).** It includes mostly parallel continuous high to medium amplitude reflections with broad frequencies. It is dissected by multiple normal faults.

Seismic Facies 4 (Sf4) is predominantly observed along the northwestern margin of the basin, occurring directly above a low-angle detachment fault. The reflections within this facies are subparallel and discontinuous. Amplitudes vary significantly and may locally reach very high values. Frequencies also exhibit considerable variability.

The Upper Badenian Seismic Sequence (lower Serravallian) (UBS) is defined by a concordant boundary at its base and an erosional boundary at its top, marked by a prominent canyon incision

Seismic Facies 5 (Sf5) corresponds to **Interval of Interest 3 (Ii3)**. This interval is characterized by a facies predominantly consisting of, high-amplitudes, fully continuous reflector with broad frequency characteristics. The high amplitudes transition to moderate or low values southeast of the boundary between the basin fill and the antithetic fault system.

Seismic Facies 6 (Sf6), corresponding to **Interval of Interest 4 (Ii4),** is characterized by indistinct prograding clinoforms with low to medium amplitudes and moderate frequency.

Seismic Facies 7 (Sf7) corresponds to **Interval of Interest 5 (Ii5**). This interval is characterized by multiple high-amplitude, fully continuous reflectors with broad frequencies, which are incised by a canyon at the top, located within the hanging wall of the antithetic fault zone. Similar to Sf5, the high amplitudes transition to moderate or low values at the boundary between the basin fill and the antithetic fault system.

Seismic Facies 8 (Sf8) is predominantly observed along the northwestern margin of the basin, situated directly above the low-angle detachment fault. Similar to Sf4, the reflections are subparallel and discontinuous. Amplitudes vary significantly and may be locally very high, while frequency also exhibits considerable variability.

The Sarmatian Seismic Sequence (3S) is defined by an erosional base characterized by canyon incisions and similar canyon-like incisions at its top. This sequence encompasses the final interval of interest.

Seismic Facies 9 (Sf9), corresponding to Interval **of Interest 6 (Ii6),** is characterized by subparallel, discontinuous reflections with variable frequencies and amplitudes. This facies is localized within a U-shaped structure. Amplitudes may occasionally reach very high values, particularly in proximity to the boundary of the antithetic fault zone.

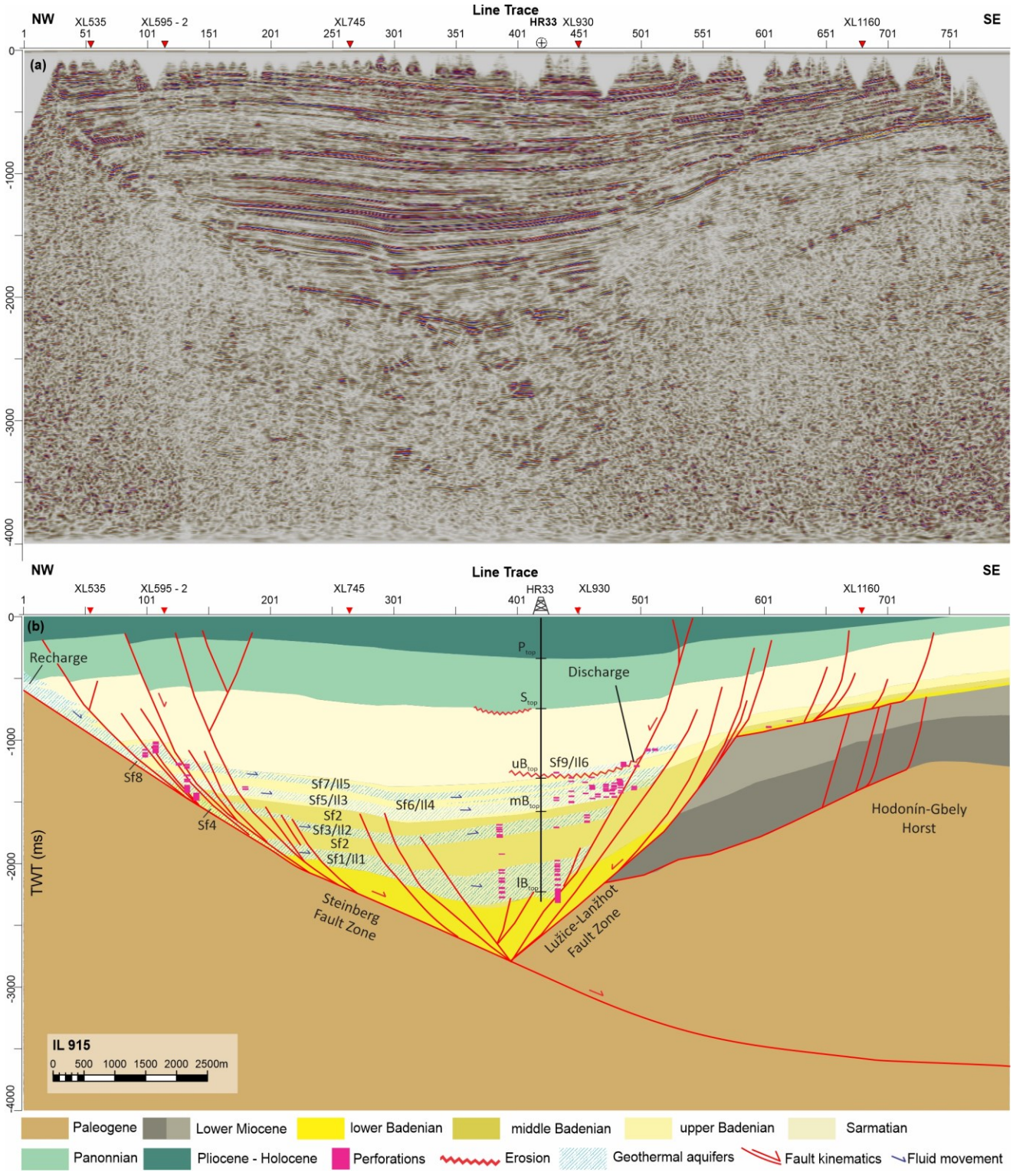

Figure 3: Geo-seismic profile IL 915. (a) Clean seismic profile with projected HR33 well (lat: 48°47'30.3609"N lon: 16°58'8.9450"E). (b) Interpreted geo-seismic profile with faults shown in red, projected well HR33, interpreted seismic sequences and facies (Sf) together with aquifer bodies in blue. See Figure 1 for location.

5. INTERPRETATION

5.1 Fault Systems and Structural Highs:

The southeast-dipping, low-angle normal fault that defines the basin margin provides compelling evidence for the final stage of tectonic evolution associated with back-arc wide-rift systems in this region. Furthermore, this fault likely serves as a major conduit for fluid migration. This interpretation is supported by several key observations. First, the fault itself, particularly its damage zone, enhances permeability and facilitates fluid flow. Second, the detachment of all faults along its upper portion, including former horse-tail faults related to strike-slip deformation, as well as subsequent antithetic and synthetic normal faults, suggests structural complexity that could further influence fluid movement. Third, the presence of debris aprons lining all of the aforementioned faults indicates active sediment transport and accumulation, likely influenced by fault-driven topographic relief. Fourth, the occurrence of alluvial fans and other sedimentary deposits cascading down fault slopes into the basin further supports the interpretation of an active sedimentary and hydrological system associated with the fault. Lastly, observations indicate that the fault extends upward at least to the top of the Pannonian (Tortonian) strata, and possibly even higher. This upward extension facilitates the development of an effective recharge zone, particularly in areas where the fault tip approaches the surface. Collectively, these factors contribute to the high effectiveness of the recharge area, which is relatively elongated and follows the northwestern flank of the basin.

The offset along the low-angle normal fault has resulted in the formation of the Gbely-Hodonín Horst, a prominent basement high. This structure is bounded at its NW side by an antithetic normal fault that opposes the low-angle normal fault. The fault zone may act as a sealed (impermeable) boundary (Figure 3), creating a potential heat trap for fluids that accumulate at the tip of the hanging wall of the zone. The intercepting deep wells drilled in this area could be re-used and serve as an ideal discharge area for trapped fluids.

From a structural development perspective, the lower and middle Badenian intervals exhibit characteristics consistent with sag-fill deposits, which can be attributed to flexural loading due to the attenuated lithosphere beneath the low-angle normal fault. This interpretation provides indirect evidence of the preceding pull-apart development stage (Figure 3).

In contrast, the Sarmatian and Pannonian intervals demonstrate pronounced thickening toward the low-angle normal fault, supporting the presence of tectonic activity during the wide-rift stage. This interpretation is further reinforced by the observation that the Gbely-Hodonín Horst was completely buried during the Sarmatian stage (Figure 3).

5.2 Stratigraphic Intervals and Geothermal Potential:

The middle Badenian (upper Langhian) Seismic sequence (MBS)

Seismic Facies 1 (Sf1) / Interval of Interest 1 (Ii1) is characterized by high amplitudes, suggesting the presence of coarse-grained lithology saturated with fluids. These characteristics are consistent with the Matzen-Auersthal formations in Austria (Harzhauser et al., 2024) or the Žižkov Formation in Czechia and Slovakia (Jamrich et al., 2024). The presence of fluids has been confirmed through multiple perforations (Figures 2,3). The observed reflections align with these formations, which may contain fluvial or coastal sand dunes. These features point to marine coastal depositional environment influenced by tidal processes.

Seismic Facies 2 (Sf2) is interpreted as representing a muddy deltaic, debris-flow-dominated, or coastal depositional environment. This interpretation is supported by the presence of indistinct progradational clinoforms, transitioning into subparallel, discontinuous reflections indicative of muddy, normal marine deposits characteristic of an inner to outer shelf setting. These features are consistent with the Baden Formation (Harzhauser et al., 2024) and its equivalent, the Jakubov Formation (Jamrich et al., 2024) Intercalated by local delta fronts and/or tidal sand dunes. The low amplitudes observed suggest a lack of significant fluid content, further indicating that Sf2 may act as a potential seal for Sf1.

The high amplitudes and broad frequencies observed in **Seismic Facies 3 (Sf3) / Interval of Interest 2 (Ii2)** suggest the presence of coarse clastics saturated with fluids, a conclusion supported by fluid confirmation from multiple perforations (Figure 3). The depositional environment is interpreted as a normal marine inner to outer shelf, associated with subaqueous sediment density flows and/or coastal sands of the Baden Formation in Austria (Harzhauser et al., 2024) or its equivalent Jakubov Formation in Czechia and Slovakia (Jamrich et al., 2024).

Seismic Facies 4 (Sf4) is characterized by subparallel and discontinuous reflections, suggesting an origin associated with alluvial fan or coarse-grained deltaic deposits developing along the basin margin. Localized fluid saturation is possible and has been confirmed in certain areas, as indicated by the presence of localized high amplitudes. This facies likely plays a critical role in facilitating fluid transmission from the low-angle detachment zone into the basin, specifically into Sf1 and Sf3. The low-angle detachment fault appears to act as a conduit, enabling fluid migration from the fault zone, which serves as a recharge area where the fault reaches the surface.

Seismic Facies 5 (Sf5) corresponds to **Interval of Interest 3 (Ii3).** It is defined by high amplitudes and broad frequencies, suggesting a fine to medium grained lithology and fluid saturation. This interpretation is supported by fluid-yielding perforations observed along both margins of the basin (Figure 3). The shift to low amplitude values southeast of the boundary between the basin fill and the antithetic fault system indicates the presence of a closure and a structural trap, further corroborated by the absence of fluid-yielding perforations within the antithetic fault system. The depositional environment is interpreted as inner shelf coastal sands, corresponding to the Studienka Formation in Czechia and Slovakia (Jamrich et al., 2024) or the equivalent sands of the Rabensburg Formation in Austria (Harzhauser et al., 2024).

Seismic Facies 6 (Sf6)/ Interval of Interest 4 (Ii4) is characterized by low to moderate amplitudes, suggesting a muddy-sand to sandstone lithological composition. This also indicates that fluid presence is not generally expected. However, fluids are observed in front of the antithetic fault zone and are absent within the fault zone, similar to observations in Sf5. This facies may be interpreted as a localized periodically flooded delta plains or large tidal sand dune complex, developing within the inner shelf environment associated with the Studienka Formation in Czechia and Slovakia or the equivalent Rabensburg Formation in Austria. This facies may also, in certain locations, function as a top seal for Sf5.

Seismic Facies 7 (Sf7)/ Interval of Interest 5 (Ii5) is characterized by high amplitudes and broad frequencies, indicative of a coarse-grained lithology and fluid saturation. This interpretation is supported by fluid-yielding perforations observed at both margins of the basin (Figure 3). The absence of fluids within the antithetic fault zone suggests that this zone acts as an effective seal, forming a structural trap, at least in this specific area. The depositional environment is interpreted as inner shelf coastal sands, corresponding to the Stupava Formation (Jamrich et al., 2024).

Seismic Facies 8 (Sf8) is characterized by subparallel and discontinuous reflections, suggesting an origin associated with periodically flooded delta plains or large tidal sand dune complexes developing along the basin margin. Localized fluid saturation, as indicated by sporadic high-amplitude reflections, has been confirmed (Figure 3). This facies is likely responsible for facilitating fluid transmission from the low-angle detachment zone into the basin, particularly into Sf5 through Sf7.

Seismic Facies 9 (Sf9), corresponding to **Interval of Interest 6 (Ii6),** is characterized by a discontinuous and subparallel (chaotic) structure within a U-shaped geometry. This configuration suggests a canyon-fill. These environments are typically formed by incision into the exposed subaerial shelf during significant sea-level fall.

6. DISCUSSION

The relatively low geothermal gradient and heat flow characteristics of the Vienna Basin, particularly in comparison to the neighboring Pannonian Basin, have been well recognized since the 1960s, as e.g. highlighted by the study of Boldizsár (1968). Nonetheless, the extensive geophysical and hydrogeological data gathered over more than 100 years of hydrocarbon exploration in the Vienna Basin have significantly contributed to advancing the understanding of the basin reservoirs. With the increasing emphasis on renewable energy transitions, the geothermal prospects of the Vienna Basin are now in high demand.

In the Austrian sector of the Vienna Basin, recent studies have focused on utilizing a Lower Miocene fluvial conglomerate aquifer to supply geothermal heat to the city of Vienna (Sachsenhofer et al., 2023). Similarly, another study has proposed the development of a geothermal field to meet the heating needs of Vienna city (Knezevic et al., 2023). Comparable formations exist in the study area of this research. However, they differ slightly in facies type, extent, and data availability thus were not considered.

Another known geothermal system in the Vienna Basin involves hot fluids ascending along major faults in the southern part of the basin. These systems have been utilized for balneological purposes since Roman times. The given fault-related geothermal system shares similarities with the setting described in this study, particularly in being located along a major basin-bounding fault zone. However, the system also includes a fluid circulation mechanism associated with deeply buried, highly permeable carbonate rocks within the Alpine wedge, specifically the Hauptdolomite Formation (which is absent in the Czech portion of the basin). This is combined with clastic reservoirs within the Neogene basin fill (Sachsenhofer et al., 2023). In contrast, the clastic reservoirs are present in the Czech part of the basin and are comparable to the geothermal systems described in this study.

Based on the seismic stratigraphy the following geothermal system can be described in the Czech part of the basin. It includes multiple geothermal reservoir aquifers represented by six intervals of interest. These intervals consist of coarse-grained formations, including the middle Badenian (upper Langhian) Matzen-Auersthal/Žižkov formations (Harzhauser et al., 2020, 2024; Jamrich et al., 2024), coastal clastic intercalations of the upper Badenian age (lower Serravallian) belonging to the Studienka/Rabensburg formations (Harzhauser et al., 2020, 2024; Jamrich et al., 2024), and the coarse clastic canyon-fill fluvial/alluvial deposits of Sarmatian age (upper Serravallian).

The reflection seismic data also reveal that these stratigraphic units are interconnected through a low-angle, basin-controlling normal fault zone known as the “Steinberg Fault Zone” (Jelínek et al., 2009), which acts as the primary recharge area. After a gradual descend along the fault zone, the fluids then migrate through the coarse-grained alluvial and deltaic facies developed at the northwestern basin margin and are subsequently transmitted into the aforementioned stratigraphic intervals. These intervals are ultimately sealed against the hanging wall of an antithetic fault zone, the “Lužice-Lanžhot Fault Zone” (Jelínek et al., 2009), which separates the footwall represented by the Gbely-Hodonín Horst (basement high) from the Central Moravian sub-basin (Jelínek et al., 2009; Harzhauser et al., 2020, 2024). The accumulated fluids are finally trapped in the hanging wall in its upper portion located at the tip of the antithetic “Lužice-Lanžhot Fault Zone” and can be recovered from this discharge area using existing operational deep wells.

The recharge areas are characterized by slightly lower temperatures within the same interval, while temperatures in the discharge areas are generally a few degrees higher. The temperature difference between recharge and discharge regions is 18°C at a depth of 1 km (Ledvényiová et al., 2025 – this volume). This temperature gradient corresponds to a gradual increase in total dissolved solids from the recharge zones toward the discharge areas, indicating progressive mineralization along the flow path. Further details on fluid geochemistry and inflow rates can be found in Ledvényiová et al. (2025 – this volume).

The water mineralization exhibits a significant variability across different stratigraphic intervals (Ledvényiová et al., 2025 – this volume). In the middle Badenian, TDS concentrations range from 3,400 to 18,000 ppm TDS, with fluid temperatures averaging 63.5 °C. In the upper Badenian, mineralization ranges from 5,600 to 13,600 ppm TDS, with temperatures between 58 and 64 °C. In the Sarmatian interval, TDS values range from 7,800 to 9,800 ppm, with fluid temperatures varying between 27.86 and 55.8 °C.

As a result, in needs to be taken into account that scaling issues may arise depending on the specific aquifer conditions (Zhao et al., 2023). Additionally, the relatively low fluid temperatures impose constraints on potential applications (Sanyal, 2005). While electricity generation is unlikely to be feasible (Sanyal, 2005), these geothermal waters could be effectively utilized for space heating (residential and commercial buildings) as exemplified by Sachsenhofer et al. (2023) and Knezevic et al. (2023), greenhouse agriculture, aquaculture (Skrzypczak et al., 2021), and recreational applications, such as hot springs and spa resorts (Haraldsson, and Cordero 2014).

Given these options, we recommend conducting a more detailed geothermal field study in the future, with a particular focus on assessing the feasibility of supplying heat to major towns in the area (e.g., Lanžhot, Břeclav, Hodonín, Holíč) for district heating. Additionally, the region has a dynamic agricultural sector, making it essential to engage local stakeholders to determine which agricultural applications would be most beneficial for them, such as greenhouse heating, aquaculture (fish farming) and soil heating (Johns et al., 1973; Boyd & Lund, 2003).

For future research, we propose conducting detailed geochemical and hydrodynamic modeling to evaluate fluid flow dynamics and heat storage capacity across the identified stratigraphic intervals as exemplified e.g. by Gao and Shi (2021), Shen et al. (2021) and Koltzer et al.(2023). Additionally, we recommend acquiring the full 3D seismic volume or at least more 2D arbitrary profiles to be able to assess the aquifers in all dimensions. Well testing also should be conducted to refine our understanding of fluid and thermal properties. Finally, we suggest exploring the integration of geothermal energy with other renewable energy systems, such as CO_2 (Randolph and Saar 2011) and H_2 storage (Ghazvini et al., 2019).

6. CONCLUSIONS

The Vienna Basin sensu stricto, particularly its Czech portion, developed as a pull-apart basin modified by subsequent back-arc extension. The Hodonín-Gbely Horst divides the Czech and Slovak sections, with the study area including four stratigraphic intervals: lower, middle, and upper Badenian, and Sarmatian. The basin margin is defined by a low-angle normal fault (Steinberg Fault Zone), facilitating fluid recharge, while the Lužice-Lanžhot antithetic Fault Zone acts as a discharge area.

The study identifies six potential geothermal reservoir intervals in the middle and upper Badenian, as well as the Sarmatian. These intervals consist of coarse-grained formations such as the Matzen-Auersthal/Žižkov, Studienka/Rabensburg, and Stupava formations. The temperature difference between recharge and discharge regions is 18 °C at a depth of 1 km. Fluids increase in total dissolved solids (TDS) from recharge to discharge areas, confirming progressive mineralization along the flow path.

Middle Badenian reservoirs exhibit TDS concentrations between 3,400 and 18,000 ppm, with fluid temperatures averaging 63.5 °C. Upper Badenian reservoirs have TDS ranging from 5,600 to 13,600 ppm TDS, with temperatures between 58 and 64 °C. Sarmatian aquifers have TDS values between 7,800 and 9,800 ppm, with fluid temperatures varying between 27.86 and 55.8 °C. Variability in salinity and mineralization across intervals necessitates further study of potential scaling issues.

Given the relatively low temperatures, direct electricity generation is unlikely. Possible applications include district heating for nearby towns (e.g., Lanžhot, Břeclav, Hodonín, Holíč), greenhouse agriculture, aquaculture, and spa-related tourism. The Lužice-Lanžhot Fault Zone presents a strategic location for fluid extraction using existing deep wells.

ACKNOWLEDGEMENTS

This research was supported by the Technology Agency of the Czech Republic (Technologická agentura ČR) under the TK – Program for the Support of Applied Research, Experimental Development, and Innovation THÉTA, specifically within Subprogram 2 - Strategic Energy Technologies, PID: TK05020137. The study was also funded by the EU NextGenerationEU through the Recovery and Resilience Plan for Slovakia under the project No. 09I03-03-V04-00127. Special thanks go to MND ltd. Czech Republic for allowing access to digital data repositories. Special thanks to Schlumberger Ltd. for their generous donation of a Petrel software license.

REFERENCES

Brown, L.F., Jr., and Fisher, W.L.: Seismic Stratigraphic Interpretation and Petroleum Exploration, AAPG Continuing Education Course, 16, (1980), 1-56. https://doi.org/10.1306/CE16409.

Brown, C.S., and Falcone, G.: Investigating Heat Transmission in a Wellbore for Low-Temperature, Open-Loop Geothermal Systems, Thermal Science and Engineering Progress, 48, (2024), 102352. https://doi.org/10.1016/j.tsep.2023.102352

Bjornsson, S., Juliusson, E., Davidsdottir, B., and Kristofersson, D. M.: Optimal Geothermal Resource Utilization—A Holistic Methodological Framework, Geothermics, 123, (2024), 103117. https://doi.org/10.1016/j.geothermics.2024.103117

Boyd, T. L., and Lund, J. W.: Geothermal Heating of Greenhouses and Aquaculture Facilities, Proceedings, International Geothermal Conference, Reykjavík, Iceland, Session #14, Geo-Heat Center, Oregon Institute of Technology (2003).

Boldizsár, T.: Geothermal Data from the Vienna Basin, Journal of Geophysical Research, 73(2), (1968), 613–625. https://doi.org/10.1029/JB073i002p00613

Coe, A.L. (Ed.): The sedimentary record of sea-level change, 287 pages, Cambridge University Press, (2003).

Dlabač, M., Kullmanová, A., Maheľ, M., Špička, V., Michalíček, M., and Šimánek, V., et al.: Research of the Pre-Neogene Bedrock in the Southeastern Part of the Vienna Basin, Partial Final Report, Partial Task: Oil Geology and the Prospectivity of the Carpathian Neogene Basins and Their Basement in Relation to Lithofacial Development and Tectogenesis, ÚÚG Praha, (1968), 214. (in Czech).

Esteve, C., Lu, Y., Gosselin, J. M., Kramer, R., Aiman, Y., and Bokelmann, G.: The Seismic Signature and Geothermal Potential of the Schwechat Depression in the Vienna Basin, Austria, from Ambient Noise Tomography, Geothermics, 127, (2025), 103211. https://doi.org/10.1016/j.geothermics.2024.103211

Fischer, K.C., and Veeken, P.: Seismic and Sequence Stratigraphy, Montan Universität, Leoben, (2015), 1-112.

Franko, O., Remšík, A., Fendek, M., Fusán, O., and Zvara, I.: Atlas of Geothermal Energy of Slovakia, The State Geological Institute of Dionýz Štúr, Bratislava, 1–164, (1995). (in Slovak).

Fordinál, K., Maglay, J., Nagy, A., Elečko, M., Vlačiky, M., Moravcová, M., Zlinská, A., Baráth, I., Boorová, D., Žecová, K., and Šimon, L.: New findings on the stratigraphy and lithological composition of Neogene and Quaternary sediments in the Záhorská nížina region, Geologické Práce Správy, 121, (2013), 47–87.

Ghazvini, M., Sadeghzadeh, M., Ahmadi, M. H., Moosavi, S., and Pourfayaz, F.: Geothermal Energy Use in Hydrogen Production: A Review, International Journal of Energy Research, 43(15), (2019), 8943–8963. https://doi.org/10.1002/er.4778

Gao, J., and Shi, Q.: A New Mathematical Modeling Approach for Thermal Exploration Efficiency Under Different Geothermal Well Layout Conditions, Scientific Reports, 11, (2021), Article 22930. https://doi.org/10.1038/s41598-021-02286-z

Haraldsson, I. G., and Lloret Cordero, A.: Geothermal Baths, Swimming Pools, and Spas: Examples from Ecuador and Iceland, Presented at Short Course VI on Utilization of Low- and Medium-Enthalpy Geothermal Resources and Financial Aspects of Utilization, UNU-GTP and LaGeo, Santa Tecla, El Salvador (2014).

Harzhauser, M., Theobalt, D., Strauss, P., Mandic, O., and Piller, W.E.: Seismic-based lower and middle Miocene stratigraphy in the northwestern Vienna Basin (Austria), Newslett Stratigr, 52(2), (2019), 221–247. https://doi.org/10.1127/nos/2018/0490

Harzhauser, M., Kranner, M., Mandic, O., Strauss, P., Siedl, W., and Piller, W.E.: Miocene lithostratigraphy of the northern and central Vienna Basin (Austria), Austr J Earth Sci, 113, (2020), 169–199. https://doi.org/10.17738/ajes.2020.0011

Harzhauser, M., Kranner, M., Siedl, W., Conradi, F., and Piller, W.E.: The Neogene of the Vienna Basin: A synthesis, The Miocene Extensional Pannonian Superbasin, Volume 1: Regional Geology, Special Publications, 554, Geological Society, London, (2024). https://doi.org/10.1144/SP554-2023-168

Haq, B.U., Hardenbol, J., and Vail, P.R.: Mesozoic and Cenozoic chronostratigraphy and cycles of sea level changes, Sea-Level Changes—An Integrated Approach, 42, Society of Economic Paleontologists and Mineralogists, SEPM Special Publication, Tulsa, (1988), 71–108. https://doi.org/10.2110/pec.88.01.0071

Hardenbol, J., Thierry, J., Farley, M.B., Jacquin, T., de Graciansky, P-C., and Vail, P.R.: Mesozoic and Cenozoic sequence chronostratigraphic framework of European basins, Mesozoic and Cenozoic Sequence Stratigraphy of European Basins, 60, Society for Sedimentary Geology, Special Publication, Tulsa, (1998), 3–13. https://doi.org/10.2110/pec.98.02.0003

Hók, J., Schuster, R., Pelech, O., Vojtko, R., and Šamajová, L.: Geological Significance of Upper Cretaceous Sediments in Deciphering the Alpine Tectonic Evolution at the Contact of the Western Carpathians, Eastern Alps, and Bohemian Massif, International Journal of Earth Sciences, 111(6), (2022), 1805–1822. https://doi.org/10.1007/s00531-022-02201-5

Hudačkova, N., Halasova, E., Kovačova, M., Rybar, S., and Kovač, M.: High-resolution study of the holotype locality of the CPN8 Zone (Globigerina druryi–Globigerina decoraperta), 14th Czech-Slovak-Polish Paleontological Conference and 9th Micropalaeontological Workshop MIKRO 2013, Grzybowski Foundation Krakow, (2013).

Idroes, G. M., Afjal, M., Khan, M., Haseeb, M., Hardi, I., Noviandy, T. R., and Idroes, R.: Exploring the Role of Geothermal Energy Consumption in Achieving Carbon Neutrality and Environmental Sustainability, Heliyon, 10, (2024), e40709. https://doi.org/10.1016/j.heliyon.2024.e40709

Jamrich, M., Rybár, S., Ruman, A., Kováčová, M., and Hudáčková, N.: Biostratigraphy and paleoecology of the upper Badenian carbonate and siliciclastic nearshore facies in the Vienna Basin (Slovakia), *Facies*, 70, (2024), 5, https://doi.org/10.1007/s10347-023-00679-2.

Lee, E.J., and Wagreich, M.: Polyphase tectonic subsidence evolution of the Vienna Basin inferred from quantitative subsidence analysis of the northern and central parts, Int. J. Earth Sci., 106, (2017), 687–705. https://doi.org/10.1007/s00531-016-1329-9.

Jamil, F., Shafiq, I., and Hussain, M.: A Critical Review on the Effective Utilization of Geothermal Energy, Energy & Environment, 35(1), (2023). https://doi.org/10.1177/0958305X231153969

Janák, J.: Classification of Deep Waters in the Czechoslovak Part of the Vienna Basin, MS Archive NAFTA as, (1955). (in Czech).

Jelínek, J., Honěk, J., Staněk, F., and Hoňková, K.: Study of Tectonic Pattern of the Dubňany Seam in the Czech Part of the Vienna Basin, GeoLines, 22, (2009), 32–39.

Johns, R. W., Folwell, R. J., Dailey, R. T., and Wirth, M. E.: An Economic Analysis of Selected Agricultural Uses of Warm Water in the Pacific Northwest Resulting from Electric Power Generation, Journal of Environmental Quality, 2(2), (1973), 189–193. https://doi.org/10.2134/jeq1973.00472425000200020011x

Knezevic, R. N., Siedl, W., Stern, G., and Ebner, M.: Application of Hydrocarbon Experience in Fuel Switch to Geothermal Energy: A Case Study from Vienna Basin, Proceedings, 84th EAGE Annual Conference & Exhibition (2023), 1–5. https://doi.org/10.3997/2214-4609.202310589

Koltzer, N., Bott, J., Bär, K., and Scheck-Wenderoth, M.: How Temperatures Derived from Fluid Flow and Heat Transport Models Impact Predictions of Deep Geothermal Potentials: The "Heat in Place" Method Applied to Hesse (Germany), Geothermal Energy, 11(2), (2023). https://doi.org/10.1186/s40517-023-00245-7

Kohl, T., and Speck, R.: Electricity Production by Geothermal Hybrid-Plants in Low-Enthalpy Areas, Proceedings, 29th Workshop on Geothermal Reservoir Engineering, Stanford University, Stanford, CA (2004), 350–355. https://pangea.stanford.edu/ERE/pdf/IGAstandard/SGW/2004/Kohl.pdf

Kováč, M., Sliva, Ľ., Sopková, B., Hlavatá, J., and Škulová, A.: Serravallian sequence stratigraphy of the Vienna Basin: High-frequency cycles in the Sarmatian sedimentary record, Geol Carpath, 59(6), (2008), 545–561.

Krijgsman, W., and Piller, W.E.: Regional stages. Central and Eastern Paratethys, A Geologic Time Scale 2012, Elsevier, Amsterdam, (2012), 935–937.

Ledvényiová, L., Nemčok, M., Kyselák, P., and Rybár, S.: Closer Look at Some Key Characteristics of Fluids in the Low-Temperature Geothermal System of the Vienna Basin – Czech Part, Proceedings, 50th Workshop on Geothermal Reservoir Engineering, Stanford University, Stanford, California, (2025), SGP-TR-229.

Matenco, L., and Radivojević, D.: On the Formation and Evolution of the Pannonian Basin: Constraints Derived from the Structure of the Junction Area Between the Carpathians and Dinarides, Tectonics, 31(6), (2012), TC6007. https://doi.org/10.1029/2012TC003206

Majorowicz, J., and Grasby, S. E.: Deep Geothermal Energy in Canadian Sedimentary Basins vs. Fossil-Based Energy We Try to Replace – Exergy [KJ/KG] Compared, Renewable Energy, 141, (2019), 259-277. https://doi.org/10.1016/j.renene.2019.03.098

Mullane, M., Gleason, M., McCabe, K., Mooney, M., Reber, T., and Young, K. R.: An Estimate of Shallow, Low-Temperature Geothermal Resources of the United States, Presented at 40th Geothermal Resources Council Annual Meeting, Sacramento, CA (2016). https://www.nrel.gov/docs/fy17osti/66461.pdf

Němec, F., and Kocák, A.: Pre-Neogene Basement of the Slovak Part of the Vienna Basin, Mineralia Slovaca, 8, (1976), 481-560. (in Czech).

Nemčok, M., Doré, A. G., Doran, H., and Henk, A.: Strike-slip terrains and transform margins: structural architecture, thermal regimes and petroleum systems, Cambridge University Press, Cambridge, 733 pp, (2024), ISBN 9781316513958, https://doi.org/10.1017/9781108686631.

Pellegrini, C., Patruno, S., Helland-Hansen, W., and Steel, R.J.: Clinoforms and Clinothems: Fundamental Elements of Basin Infill, Basin Research, 32, (2020), 185-205. https://doi.org/10.1111/bre.12446.

Randolph, J. B., and Saar, M. O.: Combining Geothermal Energy Capture with Geologic Carbon Dioxide Sequestration, Geophysical Research Letters, 38, (2011), L10401. https://doi.org/10.1029/2011GL047265

Rybár, S., Šarinová, K., Sant, K., Kuiper, K.F., Kováčová, M., Vojtko, R., Reiser, M.K., Fordinál, K., Teodoridis, V., Nováková, P., and Vlček, T.: New $^{40}Ar/^{39}Ar$, fission track and sedimentological data on a middle Miocene tuff occurring in the Vienna Basin: Implications for the north-western Central Paratethys region, Geologica Carpathica, 70(5), (2019), 386–404. https://doi.org/10.2478/geoca-2019-0022

Sachsenhofer, R. F., Misch, D., Rainer, T., Rupprecht, B. J., and Siedl, W.: The Vienna Basin: Petroleum Systems, Storage, and Geothermal Potential, Geological Society, London, Special Publications, 555(1), (2024). https://doi.org/10.1144/SP555-2023-205

Sant, K., Kuiper, K.F., Rybár, S., Grunert, P., Harzhauser, M., Mandic, O., Jamrich, M., Šarinová, K., Hudáčková, N., and Krijgsman, W.: $^{40}Ar/^{39}Ar$ geochronology using high-sensitivity mass spectrometry: Examples from middle Miocene horizons of the Central Paratethys, Geologica Carpathica, 71(2), (2020), 166–182. https://doi.org/10.31577/GeolCarp.71.2.5

Sanyal, S. K.: Classification of Geothermal Systems—A Possible Scheme, Proceedings, Thirtieth Workshop on Geothermal Reservoir Engineering, Stanford University, Stanford, CA (2005), 85–88. https://pangea.stanford.edu/ERE/pdf/IGAstandard/SGW/2005/sanyal1.pdf

Shawky, A., El-Anbaawy, M. I., Soliman, R., Shaheen, E. N., Osman, O. A., Abdel Hafiez, H. E., and Shallaly, N. A.: Utilization of Abandoned Oil Well Logs and Seismic Data for Modeling and Assessing Deep Geothermal Energy Resources: A Case Study, Science of the Total Environment, 946, (2024), 174283. https://doi.org/10.1016/j.scitotenv.2024.174283

Shen, J., Chen, M., Li, S., Cui, Z., Yuan, Y., and Feng, B.: Study on the Mechanism of Water and Heat Transfer in Sandstone Geothermal System: A Case Study of Doublet Well, Lithosphere, 2021, (2021), Article ID 5316473, 20 pages. https://doi.org/10.2113/2021/5316473

Skrzypczak, R., Kępińska, B., Pająk, L., and Bujakowski, W.: Prospects for the Application of Geothermal Resources in Agriculture in Poland, Taking Account of the Natural Functions of the Countryside, Geothermal Energy, 9(23), (2021). https://doi.org/10.1186/s40517-021-00205-z

Šarinova, K., Hudačkova, N., Rybár, S., Jamrich, M., Jourdan, F., Frew, A., Mayers, C., Ruman, A., Subova, V., and Sliva, Ľ.: $^{40}Ar/^{39}Ar$ dating and palaeoenvironments at the boundary of the early-late Badenian (Langhian-Serravallian) in the northwest margin of the Pannonian Basin system, Facies, 67, (2021), 29. https://doi.org/10.1007/s10347-021-00637-w

Špička, V.: Palaeogeography and tectonogenesis of the Vienna Basin and contribution to its oil-geological problematics, Rozpravy Československé Akademie Věd Řada Matematických- Přírodopisných Věd, 76(12), (1966), 1–118. (In Czech)

Osborn, G.: Recognition of Crustal Extension in the Basin and Range Province: A History, Geosphere, 20(5), (2024), 1247–1275. https://doi.org/10.1130/GES02758.1

Vass, D.: Lithostratigraphic units of West Carpathians: Neogene and Buda Paleogene, GUDŠ, Bratislava, (2002). (In Slovak with English summary)

Wade, B.S., and Bown, P.R.: Calcareous nannofossils in extreme environments: The Messinian Salinity Crisis, Polemi Basin, Cyprus, Palaeogeogr Palaeoclimatol Palaeoecol, 233, (2006), 271–286. https://doi.org/10.1016/J.PALAEO.2005.10.007

Zhao, H., Huang, Y., Deng, S., Wang, L., Peng, H., and Shen, X.: Research Progress on Scaling Mechanism and Anti-Scaling Technology of Geothermal Well System, Journal of Dispersion Science and Technology, 44(9), (2023), 1657–1670. https://doi.org/10.1080/01932691.2022.2033625